Lab on a Chip

Cite this: *Lab Chip*, 2011, **11**, 2948

www.rsc.org/loc

PAPER

Reaction–diffusion phenomena in a PDMS matrix can modify its topography†

Christophe Provin* and Teruo Fujii

Received 11th March 2011, Accepted 8th June 2011
DOI: 10.1039/c1lc20218a

Various reagents and solvents can be absorbed into polydimethylsiloxane (PDMS), which may be a concern for many applications. We hypothesize that these absorbed reagents can also react with each other within the elastomer matrix. Here we demonstrate this phenomenon and use it as a means to physically modify the surface topography of the PDMS by generating wrinkles or pores.

Introduction

Rubber materials such as polydimethylsiloxane (PDMS) are widely used in various fields, including microfluidics,[1] membrane separation process,[2] and both in *in vivo*[3] and *ex vivo*[4] medical devices. In addition to possessing qualities such as optical transparency, biocompatibility, and moldability, PDMS is resistant against most aqueous reagents and alcohol solvents, including ethanol. However, resistant materials are not necessarily inert, and the applications of PDMS may be more limited than previously recognized.[5] Indeed, organic solvents such as xylene are able to swell this elastomer,[6] and hydrophobic molecules can adsorb onto PDMS surfaces and be absorbed into it,[7] which is a problem for some biochemical applications.[8] In addition, PDMS is permeable to small gas molecules such as H_2, CH_4, and CO_2.[9] It is therefore reasonable to assume that absorbed reagents may be able to react together inside a PDMS matrix, in a way similar to reaction–diffusion in hydrogels.[10,11] We propose that unexpected phenomena such as unusual appearance, changes in color, and other phenomena that are sometimes observed while working with PDMS are often mistakenly regarded as indications of the presence of impurities of the material, though they may in fact arise from diffusion and reaction of species within the elastomer matrix. This possibility has not been previously investigated. Here, we show that dilute acids (nitric, hydrochloric, and acetic acid) and a dilute base (ammonia) can be absorbed by a PDMS matrix and diffuse and react within the matrix, a process that leads to topographical modifications appearing as wrinkles or pores with controllable characteristics. Our results will help with choosing reagents that are compatible with PDMS. Furthermore, we anticipate that other types of reactions or reagents than those described here would add new functionalities to elastomer materials.

Institute of Industrial Sciences, The University of Tokyo, Center for International Research on MicroMechatronics, 4-6-1-FW601, Komaba, Meguro-ku, Tokyo, 153-8505, Japan. E-mail: cprovin@iis.u-tokyo.ac.jp
† Electronic supplementary information (ESI) available: Fig. S1–S6 and data S1. See DOI: 10.1039/c1lc20218a

Results

As seen in Fig. 1, alternating and repeated injections of dilute ammonia and acid solutions (0.5 M) into a PDMS microchannel (Fig. 1a) alter the surface aspect of the PDMS surface. In the case of strong acids (nitric acid in Fig. 1b and hydrochloric acid in Fig. 1c), this alteration manifests itself as a wrinkled pattern with a homogeneous spatial wavelength λ (the feature size of the wrinkles) that can be increased from 2 to 4 μm by increasing the contact time of the hydrochloric acid and PDMS (Fig. 1c) and from 4 to 29 μm by increasing the contact time of the nitric acid and by decreasing the contact time of the ammonia (Fig. 1b). A closer look at the large wrinkles (λ of 29 μm) in the SEM picture in Fig. 2 discloses a surface aspect that is dissimilar to that in the optical micrograph in Fig. 1a, caused by the swellability of the wrinkles (ESI, Fig. S1†). It is known that wrinkles appear on PDMS as a way to release excess strain energy in response to an applied stress on a stiff thin layer supported by a soft foundation layer.[12] The wavelength follows eqn (1):[13]

$$\lambda = 2\pi h_f \left(\frac{(1-\nu_{bulk}^2)E_{film}}{3(1-\nu_{film}^2)E_{bulk}} \right)^{1/3} \quad (1)$$

where h_f corresponds to the thickness of the stiff thin film, E_{film} the Young modulus of the thin film, ν_{film} the Poisson ratio of the thin film, E_{bulk} the Young modulus of the bulk PDMS, and ν_{bulk} corresponds to the Poisson ratio of the bulk PDMS. Thus, because both the ammonia and strong acids are necessary to induce wrinkles in the PDMS (see control), these results indicate that both compounds are absorbed into the PDMS matrix and interact with each other within a thin layer whose thickness h_f depends proportionally on the contact time of the acid and is inversely proportional to the contact time of ammonia. With ammonia and acetic acid (Fig. 1d), another type of alteration appears: the formation of pores. The number of pores formed is difficult to quantify. Qualitatively, however, it appears that the number of pores formed increases with longer acetic acid contact times (as indicated by a darker color of the sidewalls of the PDMS channels, inset in Fig. 1d). The presence of pores at

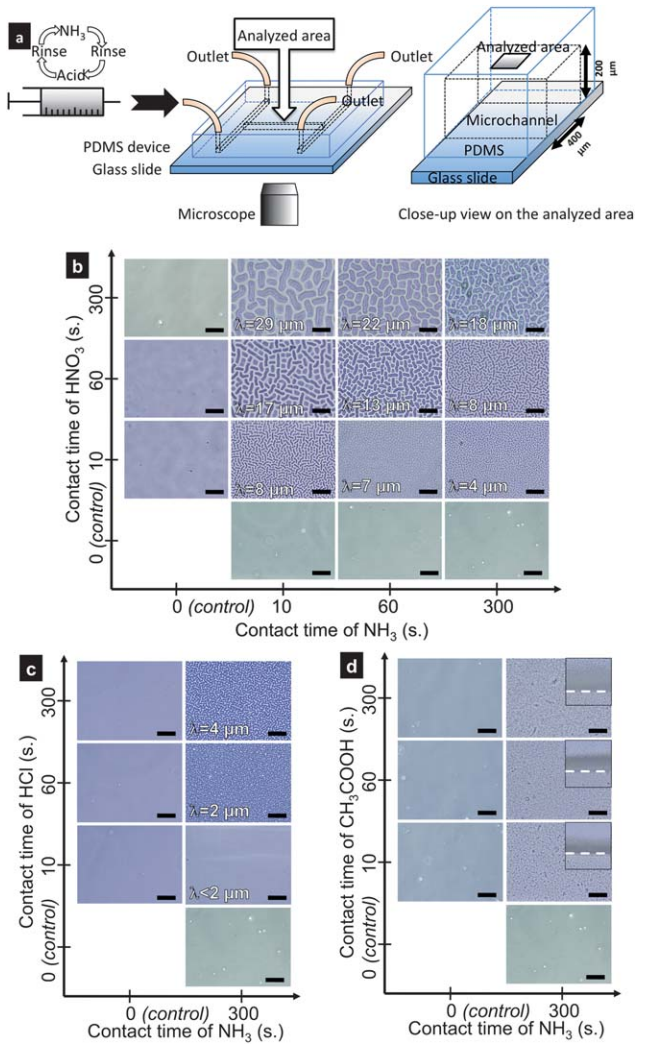

Fig. 1 Wrinkles with a controlled wavelength. (a) Schematic of the microchannel (top view) used for the repeated alternate injections of ammonia and acid. (b) Optical micrographs of PDMS channel surface showing the effect of various combinations of cycles of alternate injections of NH_3 and HNO_3 with various contact times. The channels are filled with water. (c) Same as (b) but with HCl instead of HNO_3. (d) Same as (b) but with CH_3COOH instead of HNO_3. Inset is a close-up view (170 $\times$ 170 μm^2) of the channel sidewall; the PDMS wall is above the dashed line and the water-filled channel is below. Photographs are taken once the surface appearance reaches a steady state. Scale bars represent 50 µm.

a distance of several tens of microns inside the walls demonstrates that the alteration is not exclusively a surface occurrence. Eqn (1) cannot strictly represent this phenomenon since the modified region can no longer be considered a thin film.

The FTIR surface analysis in Fig. 3 reveals the physical nature of the alteration. Indeed, no evidence of any chemical modification of the treated samples—especially grafting of amine groups (due to ammonia)[14] or oxidation (due to acids)—is present. The spectrum of the PDMS modified by ammonia in combination with weak and strong acids (Fig. 3a) shows no peaks at 3394 or 3485 cm^{-1} (primary amine N–H), or at 2206 cm^{-1} (C═N groups),[15] indicating that ammonia does not induce a chemical modification in the PDMS. The possibility of

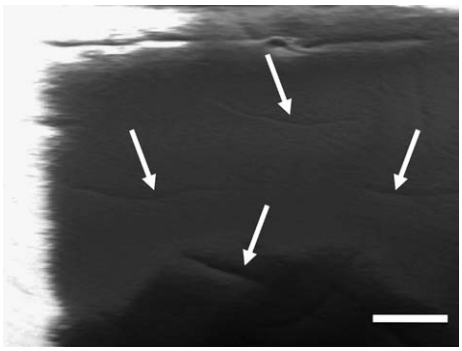

Fig. 2 Close-up view of the wrinkles. SEM picture of a few wrinkles obtained after 20 cycles of injections with a contact time of 10 s for NH_3 and 5 min for HNO_3. Wrinkles are indicated by arrows. The length of the scale bar corresponds to 20 µm.

oxidation occurring is also ruled out because no broadband absorption in the 3250–3900 cm^{-1} region, which corresponds to the OH[16,17] of silanol groups, appears (Fig. 3a) and because the CH_3–Si–O structure does not change, as evidenced by the

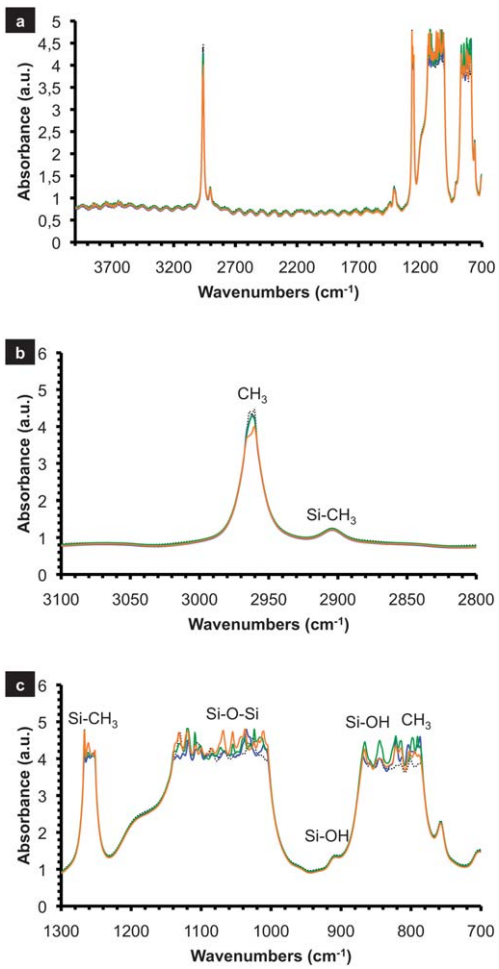

Fig. 3 FTIR absorbance spectra of 37 µm thick PDMS membranes on a Si wafer. (a) View of the whole spectrum from 4000 to 700 cm^{-1}. (b) 3100–2800 cm^{-1} range. (c) 1300–700 cm^{-1} range. Untreated PDMS (dotted line), NH_3 and HNO_3 (blue line), NH_3 and HCl (green line), and NH_3 and CH_3COOH (orange line).

Si–CH_3 (peaks located at ~2963 and 2905 cm^{-1} in Fig. 3b) and ≡Si–OH bonds (peak around 910 cm^{-1} in Fig. 3c) remaining constant for all samples. Other bands of interest,[16,18] located at approximately 1025–1265 cm^{-1} and 800–865 cm^{-1}, are in regions that are too noisy to permit reliable analysis. A noticeable decrease in the absorbance of the CH_3 peak for the sample treated with ammonia and acetic acid exists but is not corroborated by any additional evidence. The absence of chemical modification suggests that the reactions described here produce wrinkles *via* significantly different mechanisms than other processes that generate wrinkles in PDMS, which rely on the presence of a thin oxidized top layer.[17,19–28] These findings also indicate that the rugosity induced by the wrinkles is responsible for the slight increase in the contact angle from 97.6 ± 3.9° for bare PDMS to 105.8 ± 1.1° and 106.5 ± 4.3° for the nitric and hydrochloric acid-modified PDMS materials, respectively.

In Fig. 4, we further investigate the possibility of absorption in the rubber matrix using two distinct streams of ammonia and acid solutions in microchannels separated by a vertical PDMS membrane (Fig. 4a) with thicknesses increasing from 50 to 170 and finally 280 μm along the channels. Wrinkles appear in the acid channel for both strong acids, implying that ammonia diffuses through the PDMS. Indeed, gaseous ammonia is able to diffuse quickly and deeply (diffusion coefficient in PDMS, $D_{NH_3}^{PDMS} = 2.1 \times 10^{-10}$ m^2 s^{-1} (ref. 29) as compared to $D_{NH_3}^{H_2O} \approx 2 \times 10^{-9}$ m^2 s^{-1} in water)[30] within the PDMS matrix. The wavelength of the wrinkles caused by nitric acid (Fig. 4b) varies slightly across the channel, from ~15 μm near the wall close to the ammonia stream to a steady ~22 μm at one half-width from the edge of the channel. When the concentration is increased four times (Fig. 4c), no wrinkles appear on the top of the channel, but some alterations are nonetheless visible inside the PDMS at the Y-shaped reagent inlet and outlet (inset in Fig. 4c). This observation demonstrates that strong acid solutions are able to diffuse through the PDMS matrix, which is unexpected since this material has a low permeability to ions. There are, however, reports[31,32] of significantly enhanced permeability of charged species through PDMS using an ion-pair approach, an observation that may explain our results. Another hypothesis is that the element that is diffusing is the undissociated acid present in solution in exceedingly small amounts because the vapor of each strong acid may be readily able to permeate PDMS.[33] For hydrochloric acid (Fig. 4d), the wavelength along or across the channel is again smaller than that obtained with nitric acid and is relatively uniform at approximately 7 μm. Increasing the concentration of HCl (Fig. 4e) generates a gradient of wavelengths, but no alteration appears inside the PDMS membrane, suggesting that this reagent may have a lower diffusion coefficient than nitric acid in PDMS. With acetic acid (Fig. 4f), pores appear inside the PDMS membrane, confirming the easy absorption and diffusion of both ammonia and weak acids in the matrix. The increased ability of acetic acid,[34] compared to strong acids, to permeate the matrix, is probably due to its low degree of dissociation, which leads to an increased concentration of acid within the PDMS, which could explain the more dramatic tendency of this acid to release the material's internal stress as pores instead of wrinkles. The resulting porosity is significant and can deform the 50 μm wide membrane (Fig. 4f, left). A SEM image (Fig. 5) of a transversal cut of the membrane confirms the spongy nature of the acetic acid-treated PDMS, with a minimum pore diameter of approximately 1 μm. The location of the alterations is controlled by the acid concentration as an increase displaces the pores closer to the ammonia stream (Fig. 4g). Thus, ammonia, as well as nitric, hydrochloric, and acetic acids, is able to permeate the silicone rubber. As the extent of the penetration through the PDMS strongly depends on the nature of the acid, we can qualitatively rank the permeability (the product of the PDMS solubility coefficient multiplied by the diffusion coefficient)[2] of each reagent in PDMS ($\Psi_{Reagent}^{PDMS}$) in this order: $\Psi_{NH_3}^{PDMS} > \Psi_{CH_3COOH}^{PDMS} \gg \Psi_{HNO_3}^{PDMS} > \Psi_{HCl}^{PDMS}$.

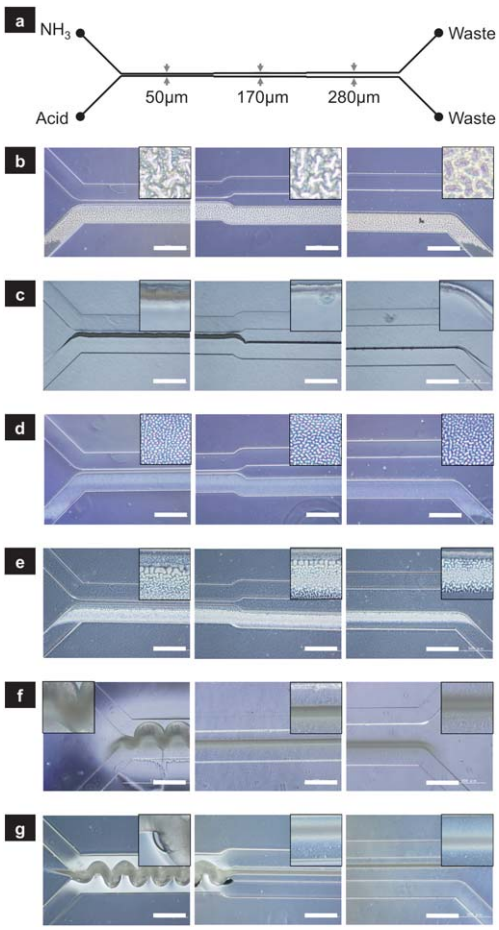

Fig. 4 Wrinkling/pores induced by diffusion of the reagents through the PDMS. (a) Schematic of the PDMS microdevice (top view) used to test the ability of the reagents to interact through a PDMS vertical membrane. The membrane width increases from 50 to 170 and finally 280 μm. The channels are filled with water. (b) Optical micrographs of the channels through which NH_3 at 0.5 M (top) and HNO_3 at 0.5 M (bottom) were allowed to flow during one hour for each membrane width. Insets are a close-up view (125 × 125 $μm^2$) of the wrinkles/pores. (c) Same as (b) but with a 2 M HNO_3 concentration. (d) Same as (b) but with HCl instead of HNO_3. (e) Same as (b) but with a 2 M HCl concentration. (f) Same as (b) but with CH_3COOH instead of HNO_3. (g) Same as (b) but with a 2 M CH_3COOH concentration. Scale bars: 500 μm.

Because the generation of wrinkles and pores relies on the quantity of reagents that diffuse, the position and intensity of the alteration are functions of the concentration in the feeding streams. This relationship is outlined in Fig. 6, where

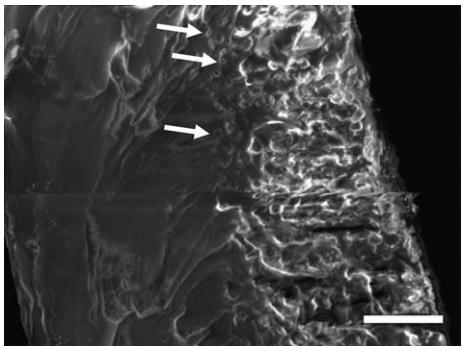

Fig. 5 SEM cut view of the pores in the 50 μm membrane from Fig. 4f. NH_3 was allowed to flow through the left channel (left side of the picture) and CH_3COOH through the right channel (right side of the picture). Arrows indicate selected small pores. The scale bar corresponds to 10 μm.

a side-by-side laminar flow of ammonia and acid streams (Fig. 6a) generates smooth mixing by diffusion alone, producing inhomogeneous alterations in the elastomer matrix. These alterations include a pattern structure with a gradient of wavelengths at the interface of the streams of ammonia and nitric acid (Fig. 6b), with λ values quickly increasing from less than 2 to 16 μm as a function of the distance from the ammonia stream. With hydrochloric acid, a broader range of structures appears (Fig. 6c) featuring straight wrinkles several hundreds of microns long along the flow path and smaller wrinkles with homogeneous wavelength. Concerning acetic acid (Fig. 6d), the pores are concentrated mainly at the interface of the two streams but can also be observed on the acid side. An interesting point is that a periodic pattern with $\lambda \approx 50$ μm (highlighted by arrows in Fig. 6d) exists in the direction of flow. The position and the intensity of the alterations for all acids are also influenced by the [ammonia]/[acid] ratio (Fig. S2 in the ESI†).

The origin of the ammonia–acid interaction is revealed in Fig. 7: the embedded pH dye sensor is yellow in the pore zone (pH < 6.8) but fuchsia in the zone between the pores and the ammonia stream (pH > 8.2), which indicates a neutralization reaction between an acid and a base within the PDMS matrix at the position where the alterations are observed.

Thus, the mechanism implies a reaction–diffusion system in PDMS that could occur according to the following scenario: ammonia and acids permeate the PDMS, but less easily for acids than for ammonia. The quantity of reagents that can permeate the material is dependent on the concentration of the feed stream or on the contact time, and on their consumption by reaction. It obeys reaction–diffusion equation (eqn (2)):

$$\frac{\partial C}{\partial t} = D_{\text{Reagent}}^{\text{PDMS}} \Delta C + R_{\text{Reagent}} \quad (2)$$

where C is the concentration of the reagent of interest in the PDMS; $D_{\text{Reagent}}^{\text{PDMS}}$ corresponds to the diffusion coefficient of the reagent in PDMS; Δ is the Laplace operator; and R_{Reagent} is the acid–base reaction term which corresponds to (eqn (3)):

$$R_{\text{Reagent}} = kCC' \quad (3)$$

where k is the kinetic constant and C' is the concentration of the second reagent.

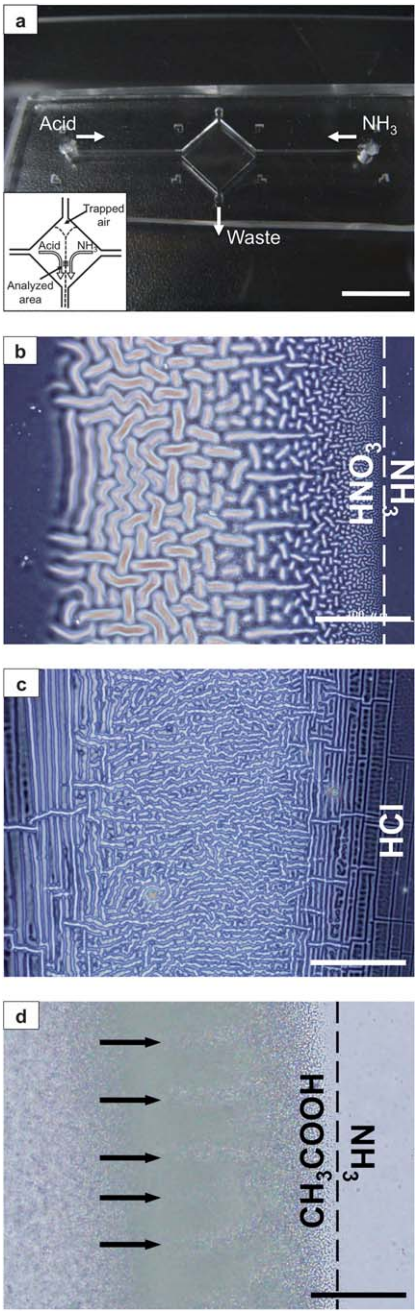

Fig. 6 Wrinkle structures obtained at the interface of two laminar streams of the reagents. (a) Photograph of a PDMS microdevice used with side-by-side laminar streams of NH_3 and acid. Inset depicts a stylized flow pattern. The scale bar corresponds to 1 cm. (b) Optical micrograph of the structure observed at the interface of two streams of reagents allowed to flow side-by-side. The device is filled with water. The HNO_3 stream is on the left of the dashed line, and the NH_3 is on the right. (c) Same as (b) but obtained using HCl instead of HNO_3. The dashed line representing the stream interface is off to the right of the micrograph. (d) Same as (b) but obtained using CH_3COOH instead of HNO_3. Arrows indicate a periodic pattern. Scale bars: 100 μm.

When the ammonia and acid come into contact, an acid–base reaction quickly occurs. The reagents are then replenished by diffusion. We can only hypothesize with regard to the subsequent steps: salts of ammonium nitrate, chloride, or acetate are formed

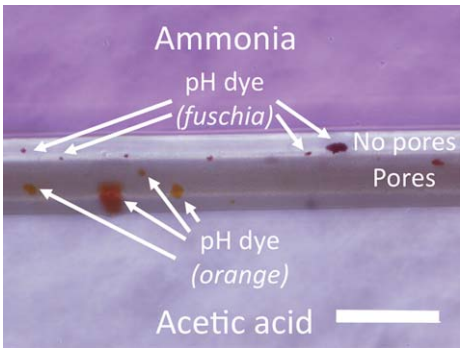

Fig. 7 Change of color of the embedded pH dye sensor when pores are generated. Optical micrograph of a 50 μm wide PDMS membrane with an embedded pH dye sensor between two channels filled with NH_3 (top) and CH_3COOH (bottom) after 30 min of reaction. Yellow color indicates pH < 6.8, fuchsia pH > 8.2, and orange corresponds to intermediate values between these two pH values. The device used in this experiment has the same design as that depicted in Fig. 4. The scale bar corresponds to 100 μm.

and become trapped in the PDMS in a region of thickness h_f. The presence of trapped salts in the PDMS modifies the mechanical properties in this region[35,36] and likely generates some stress. This stress in a small region with a different Young modulus is then released as wrinkles or pores. In addition, it is also plausible that as water can diffuse quickly ($D_{H_2O}^{PDMS} \approx 10^{-9}$ m^2 s^{-1}) through the PDMS,[37,38] it is absorbed by the salts, creating pockets of dissolved salt and generating an osmotic pressure in the silicone rubber.[39] In that case, wrinkles and pores would be generated by the stress caused by this osmotic pressure. It is also reported[39] that excessive osmotic pressure can generate micro-pipes between the swollen pockets filled with dissolved salt and the surrounding water, which may explain some observations (swelling of the wrinkles in Fig. S1†, and the presence of salts on the surface of PDMS in Fig. S5 and S6 in the ESI†).

The experimental results can be qualitatively explained with the scenario above. In Fig. 1 for repeated alternating injections of the reagents, the ammonia concentration inside the PDMS is higher than the acid concentration due to its higher permeability. Acids are thus the *de facto* limiting reagents in this system. In the case of high contact time of ammonia, the acid able to permeate reacts immediately with the ammonia absorbed near the surface and is depleted before penetrating deeper, leading to a small h_f and wrinkles with a small λ. h_f depends on the balance between each of the absorbed reagents, and therefore λ increases if the acid contact time increases or if the ammonia contact time decreases. When the streams of acid and base are distinct such as in Fig. 4, the PDMS membrane limits diffusion between the solutions. Because $D_{NH_3}^{PDMS}$ is high, ammonia is hardly blocked by the membrane, in contrast with the acids. Therefore, the only modifications appear in the acid channel for strong acids or in the membrane for acetic acid and nitric acid at 2 M because the higher concentration increases the diffusive flux. In the case of interdiffusion of the reagents in a laminar flow, *e.g.*, in Fig. 6, due to the fast acid–base reaction, the concentration in solution of each species is minimal at the interface of the two streams and increases gradually with distance. The precise location of the reaction interface depends on the initial concentrations and diffusion coefficients of the species in solution. In the PDMS, the concentration profile matches the one in solution, except that ammonia is able to diffuse much more easily through the elastomer than the acid. The reaction interface in PDMS is then located farther within the acid side. The region in which patterns appear is located between the reaction fronts in solution and in the PDMS, *i.e.* the zone in which the acid solution is above the PDMS containing diffused ammonia. The concentration gradient in this region leads to a gradient of h_f and λ, with large wavelengths occurring far from the ammonia stream and becoming shorter as the distance to the interface decreases. However for acids with a low permeability in PDMS (*i.e.* hydrochloric acid), only wrinkles with a large wavelength can appear far from the interface within the acid side. Closer to the interface, the acid cannot diffuse deep enough for small wavelength wrinkles to be observable.

Discussion

Reagents such as ammonia and acids can permeate and react in the PDMS matrix leading to a change in the topography of the material, presumably due to a change in osmotic pressure. As the reaction–diffusion process between different reagents is usually described in an aqueous medium (aqueous solution or hydrogels),[10,11,40,41] but not within a solid dense network of polymer chains, PDMS may serve as an alternative reaction medium to study reaction–diffusion systems. The use of this phenomenon as a simple and inexpensive wet process to produce stable wrinkles (Fig. S3 and S4 in the ESI†) with a controlled wavelength inside sealed PDMS microchannels could find application in optics (optical reflectors[19] and microlens arrays),[20] materials (elastic modulus determination),[21] and micro/nanofluidics (particle sieving[22,23] and nanochannel fabrication[23–25]). Although we did not try to control the orientation of the wrinkles in this study, it may be possible to order them using bas-relief structures[12] as they seem to follow Poisson's effect, or by using recent wrinkling processes based on localized solvent diffusion in an oxidized PDMS layer[42,43] as they rely on osmotic pressure as a stimulus to induce wrinkling. Besides the topographical modifications, this reaction process may also be useful for more fundamental studies of the dynamics and kinetics of the wrinkling phenomenon.

The generation of pores with a diameter in the micrometre range in microfluidic channels using acetic acid is also very interesting. Indeed, the fabrication of porous elastomers is challenging because the lower mechanical strength of these materials makes it difficult to maintain their structural integrity. Thus far, methods to produce porous PDMS are based on a porogen mixed with the monomer before or during the curing step.[44–47] The proposed process has the distinctive advantages of working once the PDMS is cured and shaped, and of generating a localized porosity with diameters in the lower range attainable by other methods.

The implications of the present work are broad because there is a strong possibility that such a phenomenon occurs with other reagents, and that other types of reactions such as oxido-reduction and/or other modifications of the PDMS matrix may occur.

Methods

Material

The microfluidic devices were manufactured by conventional molding of PDMS on an SU-8 mold master. Briefly, PDMS (Sylgard 184, Dow Corning, USA) was prepared by mixing a base and a curing agent at a 10 : 1 ratio. This mixture was then degassed and subsequently cast on a Teflon-coated SU-8 mold (SU-8 2075, Microchem, USA) obtained using photolithography. After curing at 75 °C for 90 minutes, holes were punched for reagent inlets and outlets and the PDMS part was bonded to a glass slide (Mitsumoto, Japan) using an oxygen plasma (RIE, Samco, Japan) with a 75 W RF power for a period of 5 s to yield the final microdevice. The devices were used at least several hours after the plasma treatment. The height of the microchannels was 200 μm, and the PDMS devices were approximately 2 to 3 mm thick. NH_3 (Traceselect, Fluka), HNO_3 (Cica, Japan), HCl (Sigma, analytical grade, Japan), and CH_3COOH (Traceselect, Fluka) were diluted in Milli-Q water (Millipore, Japan) to final concentrations of 0.125, 0.5, and 2 mol L^{-1}. Unless stated otherwise, the concentration of the reagents was 0.5 mol L^{-1}. The embedded pH dye sensor was obtained by adding a 0.1 ratio of a suspension composed of 10% (wt) Phenol Red (Wako, Japan) in ethanol stabilized by 1% (vol) of Tween20 in the PDMS mix (*i.e.* 10 : 1 : 0.1 PDMS : curing agent : dye suspension).

Set-up and protocol

For experiments performed under laminar flow conditions, pumping was performed either using micropumps (Denso Sangyo Co., Japan) at a flow rate of 500 μL h^{-1} for each reagent or using syringe-pumps (Baby Bee, BASi, USA) at a flow rate of 480 μL h^{-1} for each reagent for a period of one hour. During the absorption experiment (alternate injection of the reagents), a manual injection of ammonia solution followed by acid solution was performed repeatedly until a stabilization of the surface occurred (*i.e.* no more noticeable modification of the surface pattern). The number of sequences needed decreased with increasing contact time and was approximately 24 sequences for an ammonia/acid contact time of 10 s, 11 for 60 s, and 6 for 300 s. More precisely, one sequence consisted of: ammonia injection (∼150 μL) for the specified period of time → ammonia extraction → water injection for rinsing (∼150 μL) → water extraction → acid injection (∼150 μL) for the specified period of time → acid extraction → water injection for rinsing (∼150 μL). The control experiments used a sequence consisting of: ammonia or acid injection → extraction → water injection, repeated for the number of sequences necessary to obtain the same total overall contact time. The observation of the neutralization reaction with the embedded pH dye was done by filling one of the channels with ammonia and the other with acetic acid (both 0.5 M) and allowing diffusion and reaction for a period of 30 minutes before an optical micrograph was taken.

Surface analysis

Optical micrographs were obtained with an Olympus UX-71 inverted microscope (Olympus, Japan). Scanning Electron Microscope images were obtained using a JEOL 5600 SEM (JEOL, Japan). Measurement of the periodicity λ was conducted on at least 9 pairs of wrinkles at various locations within the optical micrographs of the microchannels. Taking a wrinkle as a rounded rectangle, λ was taken as the half-width to half-width distance between two adjacent and ∼parallel wrinkles. For the contact angle measurements, a flat PDMS piece (∼1 × 1 cm^2, 1–2 mm high, no O_2 plasma treatment was applied) was prepared by sequential treatment: a large drop (∼150 μL) of NH_3 was applied on the surface for a period of 5 minutes, then this drop was extracted by aspiration and the surface was rinsed with water (∼150 μL), water was then aspirated and a large drop of HNO_3 or HCl was applied for a period of 5 minutes, then drawn out and rinsed by water. This sequence was carried out 6 consecutive times, giving a λ of 18 μm for HNO_3 and 4 μm for HCl. Three 5 μL drops of water were deposited on the modified surface, and pictures of the profile of the drops were taken using a digital camera through an Olympus STM6 (Olympus, Japan) optical microscope. The analysis of the contact angle was performed by a snake method using a plug-in[48] for ImageJ software (NIH, USA). The values were averaged from the measurements made on 3 drops using an error of ±one standard deviation. The FTIR analysis was conducted using a JASCO FT/IR 230 at a resolution of 2 cm^{-1} on ∼37 μm thick PDMS membranes obtained by spin-coating at 3000 rpm for a period of 30 s on top of a Si wafer, and modified by the same protocol as for contact angle measurement, followed by a thorough water rinsing.

Acknowledgements

The authors thank Prof. Akihide Hibara and Ms Mao Fukuyama (IIS, University of Tokyo) for their help with the FTIR analysis, and Dr Yannick Rondelez (LIMMS/CNRS-IIS, University of Tokyo) for useful discussions about reaction–diffusion.

References

1 S. K. Sia and G. M. Whitesides, *Electrophoresis*, 2003, **24**, 3563.
2 E. Favre, P. Schaetzel, Q. T. Nguygen, R. Clément and J. Néel, *J. Membr. Sci.*, 1994, **92**, 169.
3 K. W. Dunn, P. N. Hall and C. T. K. Khoo, *Br. J. Plast. Surg.*, 1992, **45**, 315.
4 P. C. Nicolson and J. Vogt, *Biomaterials*, 2001, **22**, 3273.
5 R. Mukhopadhyay, *Anal. Chem.*, 2007, **79**, 3248.
6 J. N. Lee, C. Park and G. M. Whitesides, *Anal. Chem.*, 2003, **75**, 6544.
7 M. W. Toepke and D. J. Beebe, *Lab Chip*, 2006, **6**, 1484.
8 K. J. Regehr, M. Domenech, J. T. Koepsel, K. C. Carver, S. J. Ellison-Zelski, W. L. Murphy, L. A. Schuler, E. T. Alarid and D. J. Beebe, *Lab Chip*, 2009, **9**, 2132–2139.
9 T. C. Merkel, V. Bondar, K. Nagai, B. D. Freeman and I. Pinnau, *J. Polym. Sci., Part B: Polym. Phys.*, 2000, **38**, 415.
10 C. J. Campbel, R. Klajn, M. Fialkowski and B. A. Grzybowski, *Langmuir*, 2005, **21**, 418.
11 B. A. Grzybowski, K. J. M. Bishop, C. J. Campbel, M. Fialkowski and S. K. Smoukov, *Soft Matter*, 2005, **1**, 114.
12 N. Bowden, W. T. S. Huck, K. E. Paul and G. M. Whitesides, *Appl. Phys. Lett.*, 1999, **75**, 2557.
13 J. Genzer and J. Groenewold, *Soft Matter*, 2006, **2**, 310.
14 P. Vondracek and A. N. Gent, *J. Appl. Polym. Sci.*, 1982, **27**, 4517.
15 K. G. Pruden and S. P. Beaudoin, *J. Vac. Sci. Technol., A*, 2005, **23**, 208.
16 Y. Berdichevsky, J. Khandurina, A. Guttman and Y.-H. Lo, *Sens. Actuators, B*, 2004, **97**, 402.
17 T.-K. Shih, J.-R. Ho, C.-F. Chen, W.-T. Whang and C.-C. Chen, *Appl. Surf. Sci.*, 2007, **253**, 9381.

18 C. de Menezes Atayde and I. Doi, *Phys. Status Solidi C*, 2010, **7**, 189.
19 J.-H. Wang, T.-K. Shih, C.-F. Chen, K.-C. Chen, C.-C. Chen, W.-T. Whang, G. S. Huang and H.-Y. Su, *Opt. Commun.*, 2008, **281**, 3953.
20 E. P. Chan and A. J. Crosby, *Adv. Mater.*, 2006, **18**, 3238.
21 C. M. Stafford, C. Harrison, K. L. Beers, A. Karim, E. J. Amis, M. R. VanLandingham, H.-C. Kim, W. Volksen, R. D. Miller and E. E. Simonyi, *Nat. Mater.*, 2004, **3**, 545.
22 K. Efimenko, M. Rackaitis, E. Manias, A. Vaziri, L. Mahadevan and J. Genzer, *Nat. Mater.*, 2005, **4**, 293.
23 D. Huh, K. L. Mills, X. Zhu, M. A. Burns, M. D. Thouless and S. Takayama, *Nat. Mater.*, 2007, **6**, 424.
24 S. Chung, J. H. Lee, M.-W. Moon, J. Han and R. D. Kamm, *Adv. Mater.*, 2008, **20**, 3011.
25 T. Ohzono, H. Monobe, K. Shiokawa, M. Fujiwara and Y. Shimizu, *Soft Matter*, 2009, **5**, 4658.
26 A. Chiche, C. M. Stafford and J. T. Cabral, *Soft Matter*, 2008, **4**, 2360.
27 J.-Y. Park, H. Y. Chae, C.-H. Chung, S. J. Sim, J. Park, H. H. Lee and P. J. Yoo, *Soft Matter*, 2010, **6**, 677.
28 E. P. Chan and A. J. Crosby, *Soft Matter*, 2006, **2**, 324.
29 L. L. Blyler, Jr, R. A. Lieberman, L. G. Cohen, J. A. Ferrara and J. B. Macchesney, *Polym. Eng. Sci.*, 1989, **29**, 1215.
30 D. G. Leaist, *J. Phys. Chem.*, 1987, **91**, 4635.
31 C. Valenta, U. Siman, M. Kratzel and J. Hadgraft, *Int. J. Pharm.*, 2000, **197**, 77.
32 V. Sarveiya, J. F. Templeton and H. A. E. Benson, *Eur. J. Pharm. Sci.*, 2005, **26**, 39.
33 M. G. Baron, R. Narayanaswamy and S. C. Thorpe, *Sens. Actuators, B*, 1996, **34**, 511.
34 L. Li, Z. Xiao, Z. Zhang and S. Tan, *Chem. Eng. J.*, 2004, **97**, 83.
35 T. Kaully, A. Siegmann and D. Shacham, *Polym. Compos.*, 2008, **29**, 396.
36 A. Goyal, A. Kumar, P. K. Patra, S. Mahendra, S. Tabatabaei, P. J. J. Alvarez, G. John and P. M. Ajayan, *Macromol. Rapid Commun.*, 2009, **30**, 1116.
37 E. Verneuil, A. Buguin and P. Silberzan, *Europhys. Lett.*, 2004, **68**, 412.
38 G. C. Randall and P. S. Doyle, *Proc. Natl. Acad. Sci. U. S. A.*, 2005, **102**, 10813.
39 R. Schirrer, P. Thepin and G. Torres, *J. Mater. Sci.*, 1992, **27**, 3424.
40 V. Castets, E. Dulos, J. Boissonade and P. De Kepper, *Phys. Rev. Lett.*, 1990, **64**, 2953.
41 R. D. Vigil, Q. Ouyang and H. L. Swinney, *Physica A*, 1992, **188**, 17.
42 J. Y. Chung, A. J. Nolte and C. M. Stafford, *Adv. Mater.*, 2009, **21**, 1358.
43 C. J. Rand, R. Sweeney, M. Morrissey, L. Hazel and A. J. Crosby, *Soft Matter*, 2008, **4**, 1805.
44 T. Kobayashi, H. Saitoh, N. Fujii, Y. Hoshino and M. Takanashi, *J. Appl. Polym. Sci.*, 1993, **50**, 971.
45 F. Arai, N. Inomata, R. Ookawara, Y. Yamanishi and Y.-C. Lin, *Proceedings of the 2007 International Symposium on Micro-NanoMechatronics and Human Science (MHS2007)*, Nagoya, 2007.
46 O. Dufaud, E. Favre and V. Sadtler, *J. Appl. Polym. Sci.*, 2002, **83**, 967.
47 M. Juchniewicz, D. Stadnik, K. Biesiada, A. Olszyna, M. Chudy, Z. Brzozka and A. Dybko, *Sens. Actuators, B*, 2007, **126**, 68.
48 F. Stalder, G. Kulik, D. Sage, L. Barbieri and P. Hoffmann, *Colloids Surf., A*, 2006, **286**, 92.

